nature aging

Brief Communication

https://doi.org/10.1038/s43587-022-00340-7

Optogenetic rejuvenation of mitochondrial membrane potential extends *C. elegans* lifespan

Received: 28 January 2022

Accepted: 22 November 2022

Published online: 30 December 2022

Check for updates

Brandon J. Berry[1], Anežka Vodičková[2], Annika Müller-Eigner[3], Chen Meng[4], Christina Ludwig[4], Matt Kaeberlein[1], Shahaf Peleg[3] ✉ & Andrew P. Wojtovich[2] ✉

Mitochondrial dysfunction plays a central role in aging but the exact biological causes are still being determined. Here, we show that optogenetically increasing mitochondrial membrane potential during adulthood using a light-activated proton pump improves age-associated phenotypes and extends lifespan in *Caenorhabditis elegans*. Our findings provide direct causal evidence that rescuing the age-related decline in mitochondrial membrane potential is sufficient to slow the rate of aging and extend healthspan and lifespan.

The causal role of mitochondrial dysfunction and metabolic decline are central questions of aging research[1,2]. The voltage potential across the inner membrane of mitochondria (membrane potential $\Delta\psi_m$) decreases with age in many model systems[3–6]. $\Delta\psi_m$ is a fundamental driver of diverse mitochondrial functions, including adenosine triphosphate (ATP) production, immune signaling and genetic and epigenetic regulation[7]. Decreased $\Delta\psi_m$ is an attractive explanation for the complex dysfunctions of aging; however, it is unclear whether decreased $\Delta\psi_m$ is a cause or a consequence of cellular aging.

To test these questions in a metazoan, we used optogenetics to harness light energy using a mitochondria-targeted light-activated proton pump to increase $\Delta\psi_m$. Using a mitochondrial targeting sequence, we previously expressed a rhodopsin-related proton-specific pump[8] in the inner membrane of mitochondria[9]. We called this tool 'mitochondria-ON' (mtON) (Fig. 1a) and previously characterized its optogenetic function[9]. mtON isolates $\Delta\psi_m$ as a single experimental variable in vivo and requires both light activation and a cofactor, all-trans-retinal (ATR), for proton pumping activity[9]. *Caenorhabditis elegans* does not produce ATR, allowing for control conditions of light exposure alone (which can be damaging[10]), mtON protein expression alone and ATR supplementation alone (which does not affect lifespan or physiology in this context; Supplementary Table 1 and previously[11]). Only animals supplemented with ATR and illuminated will have mtON activity and increased $\Delta\psi_m$ (Supplementary Fig. 1)[9].

We found that $\Delta\psi_m$ naturally declines with age in *C. elegans* (Fig. 1b,c), as expected[2,3,5]. mtON activation reversed that decline in two different genetic backgrounds (Fig. 1d and Supplementary Figs 2 and 3). mtON activation did not impact mitochondrial mass observed by mitochondrial staining and quantitative proteomics (Supplementary Fig. 3d and Supplementary Fig. 4a). Respiration rates were similar across conditions (Fig. 1e,f) as expected, given mtON's specificity for $\Delta\psi_m$ alone[9].

We activated mtON throughout lifespan beginning in adulthood and found an increase in lifespan compared to controls (Fig. 2a,b and Supplementary Fig. 1). Lifespan extension was replicated independently across three different strains, different light intensities and in different laboratories (Supplementary Table 1) and was sensitive to the mitochondrial uncoupler, carbonyl cyanide p-(trifluoromethoxy) phenylhydrazone (FCCP) (Fig. 2c), which dissipates $\Delta\psi_m$. FCCP had no effect on lifespan on its own (Fig. 2c) and ATR and light did not affect lifespan in wild-type animals (Supplementary Table 1). When exposed to light below the threshold to maximally activate mtON[9] lifespan was not extended (Supplementary Fig. 6a). These data together indicate that increasing $\Delta\psi_m$ causes increased lifespan.

[1]University of Washington, Department of Laboratory Medicine & Pathology, Seattle, WA, USA. [2]University of Rochester Medical Center, Department of Anesthesiology and Perioperative Medicine, Rochester, NY, USA. [3]Research Group Epigenetics, Metabolism and Longevity, Research Institute for Farm Animal Biology (FBN), Dummerstorf, Germany. [4]Bavarian Center for Biomolecular Mass Spectrometry (BayBioMS), Technical University of Munich, Freising, Germany. ✉e-mail: peleg@fbn-dummerstorf.de; andrew_wojtovich@urmc.rochester.edu

https://doi.org/10.1038/s43587-022-00340-7

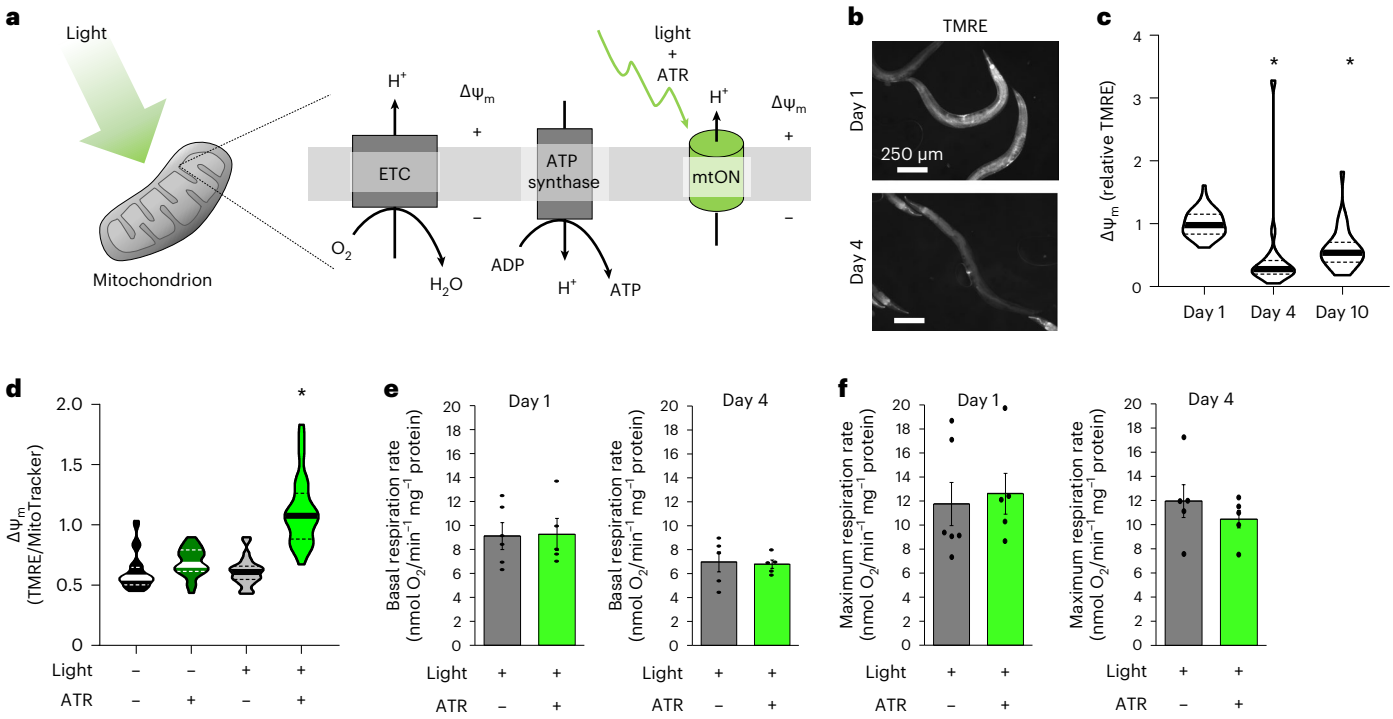

Fig. 1 | Mitochondria-ON increased $\Delta\psi_m$ in vivo. a, The mitochondrial inner membrane (IM) contains the electron transport chain (ETC), which pumps protons to generate mitochondrial membrane potential ($\Delta\psi_m$). mtON is an engineered light-activated proton pump and, in response to light and ATR supplementation, pumps protons across the IM to generate $\Delta\psi_m$. **b**, Adult worms stained with the $\Delta\psi_m$ indicator, TMRE. Scale bar, 250 µm. **c**, Quantification of relative TMRE fluorescence. One-way analysis of variance (ANOVA) with Tukey's multiple comparisons test, day 1 versus day 4, $P = 0.0001$, day 1 versus day 10, $P = 0.0002$, $n = 44$, 18 and 30. Data are median ± quartiles (dotted lines). **d**, Pharynx TMRE fluorescence normalized to mitochondrial mass in day 4 worms. One-way ANOVA with Tukey's test, all significant differences, $P = 0.0001$, $n = 33$, 34, 26 and 35 animals for each bar from left to right. Data are median ± quartiles. **e**, Basal oxygen consumption of day 1 (left) and day 4 (right) animals, no ATR $n = 5$ populations and ATR $n = 6$ populations. Data are mean ± s.e.m. Dots are individual populations. **f**, Maximal oxygen consumption (induced by FCCP) of the same populations (no ATR $n = 5$ populations and ATR $n = 6$ populations) in **h**. Data are mean ± s.e.m. Dots are individual populations.

Mild inhibition of mitochondrial function during development (but not during adulthood) extends *C. elegans* lifespan[12,13]; conversely, here, we show that attenuating the age-associated decrease in $\Delta\psi_m$ in adults can extend lifespan. Accordingly, targets of the mitochondrial unfolded protein response did not change after mtON activation (Supplementary Fig. 4b). These differences may reflect a lifespan-extending hormetic response from mitochondrial perturbation during development[14–16] versus the beneficial effects from directly sustaining mitochondrial function during adulthood[2].

Organisms, including humans and *C. elegans*, have trouble moving as they age due to physiological decline[17–19]. This functional decline was mitigated by mtON activation in worms thrashing in liquid, but not on solid media (Fig. 2d,e and Supplementary Fig. 5a–c). These results show that age-associated physiological dysfunction can be improved by reversing the loss of $\Delta\psi_m$ that occurs with age. How improving $\Delta\psi_m$ may influence redox metabolites, including NAD^+/NADH, which are known to impact biological aging, should be further assessed. To probe a potential signaling pathway, we tested the effect of mtON in long-lived worms with constitutively active AMPK signaling[20]. mtON further increased lifespan in this model (Supplementary Fig. 6b and Supplementary Table 1), indicating that increased $\Delta\psi_m$ can additionally contribute to longevity in parallel with a canonical signaling pathway.

In summary, we used a technology that harnesses light energy to generate $\Delta\psi_m$ to test the hypothesis that $\Delta\psi_m$ causally determines longevity in *C. elegans* (Fig. 2f). A limitation of this study relates to the concept of optogenetic control over mitochondria; it is unclear whether this mechanism of lifespan extension is involved in other longevity paradigms. Previous studies reported that inhibition of mitochondrial function during development can increase lifespan and our results extend the role of mitochondrial function in aging to adult intervention. Despite limitations, we show that preserved $\Delta\psi_m$ during adulthood is sufficient to slow normative aging and improve at least some functional measures of health. This work provides important context for understanding the role of mitochondrial function during aging and suggests the potential of new approaches to delay aging by targeting $\Delta\psi_m$ specifically.

Methods

All research was approved by the University of Rochester Institutional Biosafety Committee.

C. elegans strains and maintenance

Nematode growth medium (NGM) was used for *C. elegans* culture and all maintenance and experiments were carried out at 20 °C. OP50 *Escherichia coli* was used as a food source for all experiments. Where indicated, ATR and/or FCCP was added to food at a final concentration of 100 µM and 10 µM, respectively, accounting for the volume of the NGM. Egg-lay-synchronized day 1 adult hermaphrodite animals were used for all experiments unless otherwise noted. APW32 (genotype *pha-1(e2123ts)* III; *jbmEx11* (pBJB20(*Peft-3::Mitofilin(N′ 187 aa)::Mac::GFP*), pC1 (*pha-1(+)*)) expresses mtON as an extrachromosomal array[9]. APW273 (genotype *jbmSi10*(*eft-3p::Mitofilin(187 N′aa)::Mac:mKate::unc-54 3′ UTR *cxTi10816*) IV) was created using a *Mos1* element-mediated CRISPR integration approach[21]. Briefly, PCR fragments (Supplementary Table 3) were amplified and incorporated into a *Mos1* element on chromosome

https://doi.org/10.1038/s43587-022-00340-7

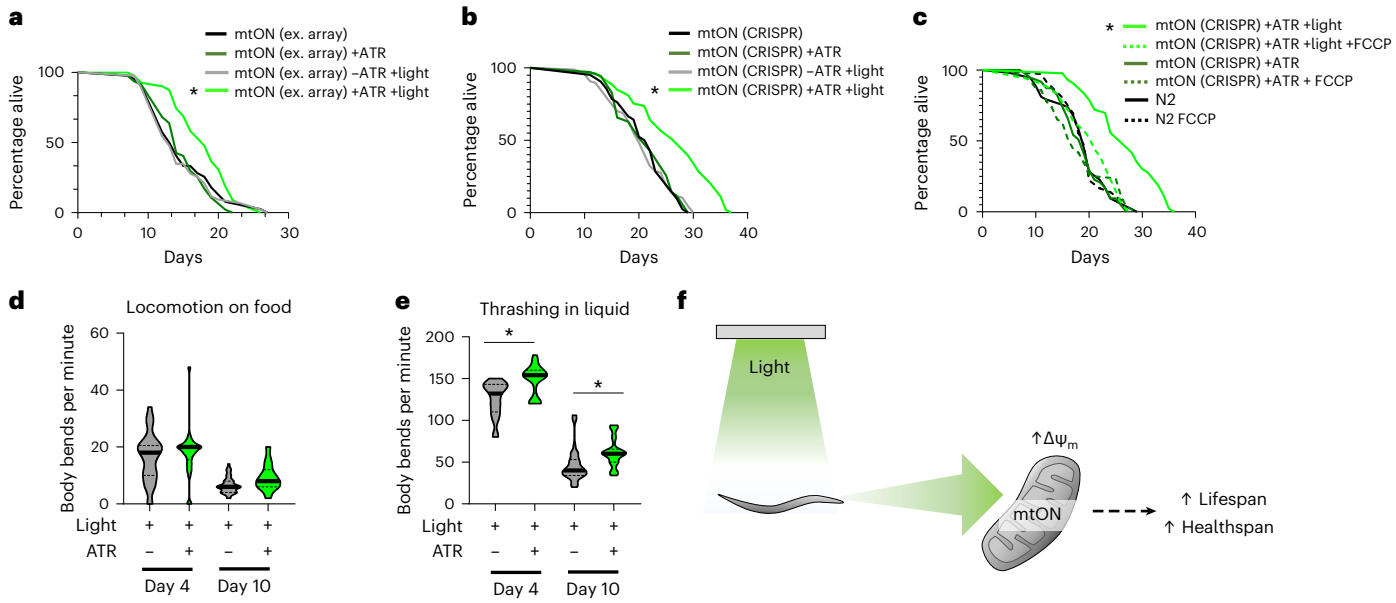

Fig. 2 | mtON extended lifespan and healthspan. Light treatment began at day 1 of adulthood for all experiments. **a**, Survival curves of mtON-expressing animals (extrachromosomal array). Only mtON activation (+ATR +light) significantly extended lifespan, log-rank (Mantel–Cox) test, *$P = 0.019$. Detailed statistical information for all lifespans is presented in Supplementary Table 1. **b**, Survival curves of mtON-expressing animals (CRISPR insertion). mtON activation significantly extended lifespan compared to the light control by log-rank (Mantel–Cox) test, *$P = 0.0001$, gray and light-green curves. **c**, Increased lifespan by mtON activation was sensitive to FCCP, log-rank (Mantel–Cox) test, $P = 0.0001$. **d**, mtON activation did not affect locomotion on solid media. One-way ANOVA with Tukey's test; $n = 30$ animals for day 4 conditions and 40 animals for day 10. Data are median ± quartiles (dotted lines). **e**, mtON activation improved mobility in liquid with age. One-way ANOVA with Tukey's test, day 10 no ATR light versus day 10 ATR light; $P = 0.002$, all other significant comparisons, $P = 0.0001$; $n = 32$, 32, 40 and 40 animals for each violin from left to right. Data are median ± quartiles. All statistical comparisons are presented in Supplementary Table 2. **f**, Model showing effects of mtON activation in vivo. The dotted arrow represents the molecular mechanisms to be investigated that link $\Delta\psi_m$ to aged physiology.

IV using CRISPR/Cas9 homology-directed repair[22]. *C. elegans* were injected with a mix containing 25 mM KCl, 7.5 mM HEPES, 4 µg µl^{-1} tracrRNA, 0.8 µg µl^{-1} *Mos1* crRNA2 (target sequence GTCCGCGTTTGCTCTTTATT), 0.8 µg µl^{-1} *dpy-10* crRNA, 50 ng µl^{-1} *dpy-10* ssODN, 2.5 µg µl^{-1} purified Cas9 and 300–400 pmol µl^{-1} of each PCR repair template fragment. APW312 (genotype *jbmSi10* IV; *uthIs248*) expresses a constitutively active AAK-2 with mtON and was generated by crossing WBM60 (genotype *uthIs248* (*Paak-2::aak-2 genomic*(*aa 1–321* with *T181D)::GFP::unc-54 3′ UTR, Pmyo-2::tdTomato*) with APW273.

In vivo mitochondrial membrane potential measurement

Animals were stained for 24 h with both 100 nM TMRE and 12 µM MitoTracker Green FM. Tetramethylrhodamine ethyl ester (TMRE) was dissolved in ethanol and placed onto seeded plates and MitoTracker Green FM was dissolved in dimethylsulfoxide (DMSO) and added to the OP50 food. Final concentrations accounted for the entire plate NGM volume. TMRE and MitoTracker Green FM were used to measure mitochondrial membrane potential and mitochondrial mass, respectively. Staining began at day 4 of adulthood and animals were transferred to plates without dye for 1 h before imaging to clear the gut of residual dye. Animals were mounted on 2% agarose pads under tetramisole (0.1% w/v) anesthesia. Texas Red and green fluorescent protein filter sets were used to record images on an epifluorescence microscope (Nikon MVX10). Images were recorded with a Lumenera camera and associated software (Infinity Analyze). Fluorescence intensity was quantified using ImageJ by drawing regions of interest around individual animals, around the head region alone or around individual pharynxes where indicated to determine their fluorescence intensity. Head region analysis served to quantify pharynx fluorescence and to specifically exclude intestinal staining as previously described[23]. Background signal was averaged and manually subtracted using ImageJ. Data are from three different experimental days. Confocal images were acquired using a Leica SP8X DMI6000 confocal microscope using a ×63 oil immersion objective and a tunable white light laser (470–670 nm). Confocal images were single optical slices and not from z-stacks or maximum projections. Images were analyzed and prepared using Leica LASX Expert software and ImageJ.

mtON activation

Illumination was carried out with a 590 nm LED array with STOmk-II stimulator by Amuza placed 2 cm away from the surface of NGM plates. Intensity was measured using a calibrated optical power meter (1916-R, Newport Corporation). Animals were exposed to 1 Hz, 0.01–2.1 mW mm^{-2} light to help maintain temperature across experiments. Under all lighting conditions mtON was maximally activated (lower limit of 0.01 mW mm^{-2} (ref. 9) unless otherwise noted. Lifespans were carried out starting at day 1 of adulthood until death or until they were removed to measure mitochondrial parameters. A digital temperature probe was used to report temperature variability across different incubators and different light sources to ensure data comparability across lifespan experiments. This was necessary due to light sources causing small local increases in temperature. All incubators were always set to 20 °C.

Whole organism respiration

Oxygen consumption rate was measured using a Clark-type oxygen electrode (S1 electrode disk, DW2/2 electrode chamber and Oxy-Lab control unit, Hansatech Instruments). Around 1,000 animals per condition, per replicate were collected in M9, allowed to settle by gravity, rinsed in M9 buffer, settled again and finally added to the electrode chamber in 0.5 ml of continuously stirred M9 buffer. FCCP was added at 160 µM final concentration in the chamber to induce maximal respiration. Respiration rates were measured for 10 min or until stable. Animals were then collected in M9 buffer for protein quantification using the Folin-phenol method.

Lifespan analysis

Animals were transferred to new plates every 2 d until reproduction ceased and as necessary to replenish food. Where indicated, 50 µM floxuridine was used in the NGM to prevent progeny from developing. Animals that did not move in response to a light touch to the head with a platinum wire were scored as dead and removed from assay plates. The 1–3 plates for each condition were scored concurrently with ~15–70 animals per plate. All experiments were performed to maintain 20 °C, which sometimes required adjustment of light intensity (noted in Supplementary Table 1). Animals were illuminated only during adulthood. FCCP was added to plates at 10 µM final concentration. This dose did not affect lifespan on its own (Supplementary Table 1; FCCP lifespan). All lifespans consisted of three biological replicates pooled for each experiment.

Locomotion assays

Synchronized animals were observed and locomotion was scored by counting body bends according to previous methods[24]. Locomotion was scored in the presence of food on solid media. Thrashing was similarly analyzed with animals placed in M9 buffer to move freely in liquid. Body bends were counted for 30 s for each animal in all cases and multiplied by two to represent body bends per min in accordance with previously used protocols[9,25]. Data are from at least three different experimental days.

Protein extraction from *C. elegans*

C. elegans were washed and stored in water after 4 d of illumination. Worms were centrifuged for 5 min at 200*g* at 4 °C and supernatant was discarded. The worm pellet was then resuspended in 100 µl Lyse (iST Sample Preparation kit, Preomics, Planegg/Martinsried), incubated at 95 °C for 10 min at 500 r.p.m. shaking and sonicated for 10 × 10 s at 30% amplitude. The sample was then centrifuged at 8,000*g* for 15 min at 4 °C and the supernatant was transferred to a new vial. The protein concentration was measured with a NanoDrop 2000.

Proteomics sample preparation

A starting material of 100 µg protein in 50 µl Lyse was recommended for the sample preparation with the Preomics iST Sample Preparation kit. In cases where protein concentration was higher than 2 µg µl^{-1}, the sample was diluted with Lyse. The preparation was performed according to supplier guidelines (iST Sample Preparation kit, Preomics, P.O.00001).

LC–MS/MS data acquisition

Liquid chromatography tandem mass spectrometry (LC–MS/MS) measurements were performed on an Ultimate 3000 RSLCnano system coupled to a Q-Exactive HF-X mass spectrometer (Thermo Fisher Scientific). Peptides were delivered to a trap column (ReproSil-pur C18-AQ, 5 µm, Dr Maisch, 20 mm × 75 µm, self-packed) at a flow rate of 5 µl min^{-1} in 100% solvent A (0.1% formic acid in HPLC-grade water). After 10 min of loading, peptides were transferred to an analytical column (ReproSil Gold C18-AQ, 3 µm, Dr Maisch, 450 mm × 75 µm, self-packed) and separated using a 110 min gradient from 4% to 32% of solvent B (0.1% formic acid in acetonitrile and 5% (v/v) DMSO) at 300 nl min^{-1} flow rate. The Q-Exactive HF-X mass spectrometer was operated in data dependent acquisition and positive ionization mode. MS1 spectra (360–1,300 m/z) were recorded at a resolution of 60,000 using an automatic gain control target value of 3×10^6 and maximum injection time of 45 ms. Up to 18 peptide precursors were selected for fragmentation for the full proteome analyses. Only precursors with charge states 2–6 were selected and dynamic exclusion of 30 s was enabled. Peptide fragmentation was performed using higher energy collision induced dissociation and a normalized collision energy of 26%. The precursor isolation window width was set to 1.3 m/z. MS2 resolution was 15,000 with an automatic gain control target value of 1×10^5 and maximum injection time of 25 ms.

LC–MS/MS data analysis

Peptide identification and quantification was performed using MaxQuant (v.1.6.3.4). MS2 spectra were searched against the Uniprot *C. elegans* proteome database (UP000001940, 26,672 protein entries, downloaded 21 December 2020) supplemented with the mKate-tagged proton pump protein plus common contaminants. Trypsin/P was specified as a proteolytic enzyme. Precursor tolerance was set to 4.5 ppm and fragment ion tolerance to 20 ppm. Results were adjusted to 1% false discovery rate on peptide spectrum match level and protein level employing a target-decoy approach using reversed protein sequences. The minimal peptide length was set at seven amino acids and the 'match-between-run' function was disabled. Carbamidomethylated cysteine was set as fixed modification and oxidation of methionine and N-terminal protein acetylation as variable modifications. The label-free quantification[26] from MaxQuant was used to represent the relative abundance of proteins across samples. ATP synthase, HSP6, HSP60, TOM70, VDAC and mitochondrial complex proteins were manually selected. The different expressions of these proteins between ATR-positive and ATR-negative samples were analyzed using a Student's *t*-test.

Statistics and reproducibility

Statistics were performed in GraphPad PRISM (v.9.3.0). No data were excluded from the analysis. No statistical method was used to predetermine sample size. Within experimental groups, animals were randomized for each experimental replicate. The investigators were not blinded to allocation during experiments and outcome assessment. Data distribution was assumed to be normal but this was not formally tested, therefore data distributions are visualized in each figure.

Reporting summary

Further information on research design is available in the Nature Portfolio Reporting Summary linked to this article.

Data availability

All other data supporting the findings of this study are available from the corresponding author upon reasonable request. The mass spectrometry proteomics data have been deposited to the ProteomeXchange Consortium (http://proteomecentral.proteomexchange.org) via the PRIDE[27–29] partner repository with the dataset identifier PXD033901.

References

1. Lopez-Otin, C. et al. The hallmarks of aging. *Cell* **153**, 1194–1217 (2013).
2. Berry, B. J. & Kaeberlein, M. An energetics perspective on geroscience: mitochondrial protonmotive force and aging. *Geroscience* **43**, 1591–1604 (2021).
3. Hughes, A. L. & Gottschling, D. E. An early age increase in vacuolar pH limits mitochondrial function and lifespan in yeast. *Nature* **492**, 261–265 (2012).
4. Hughes, C. E. et al. Cysteine toxicity drives age-related mitochondrial decline by altering iron homeostasis. *Cell* **180**, 296–310 (2020).
5. Mansell, E. et al. Mitochondrial potentiation ameliorates age-related heterogeneity in hematopoietic stem cell function. *Cell Stem Cell* https://doi.org/10.1016/j.stem.2020.09.018 (2020).
6. Ziegler, D. V. et al. Calcium channel ITPR2 and mitochondria-ER contacts promote cellular senescence and aging. *Nat. Commun.* **12**, 720 (2021).
7. Martínez-Reyes, I. & Chandel, N. S. Mitochondrial TCA cycle metabolites control physiology and disease. *Nat. Commun.* **11**, 102 (2020).

8. Waschuk, S. A. et al. Leptosphaeria rhodopsin: bacteriorhodopsin-like proton pump from a eukaryote. *Proc. Natl Acad. Sci. USA* **102**, 6879–6883 (2005).
9. Berry, B. J. et al. Optogenetic control of mitochondrial protonmotive force to impact cellular stress resistance. *EMBO Rep.* **21**, e49113 (2020).
10. De Magalhaes Filho, C. D. et al. Visible light reduces *C. elegans* longevity. *Nat. Commun.* **9**, 927 (2018).
11. Busack, I. et al. The OptoGenBox – a device for long-term optogenetics in. *J. Neurogenet.* **34**, 466–474 (2020).
12. Rea, S. L., Ventura, N. & Johnson, T. E. Relationship between mitochondrial electron transport chain dysfunction, development, and life extension in *Caenorhabditis elegans*. *PLoS Biol.* **5**, e259 (2007).
13. Ventura, N., Rea, S. L. & Testi, R. Long-lived *C. elegans* mitochondrial mutants as a model for human mitochondrial-associated diseases. *Exp. Gerontol.* **41**, 974–991 (2006).
14. Yang, W. & Hekimi, S. A mitochondrial superoxide signal triggers increased longevity in *Caenorhabditis elegans*. *PLoS Biol.* **8**, e1000556 (2010).
15. Ristow, M. & Schmeisser, S. Extending life span by increasing oxidative stress. *Free Radic. Biol. Med* **51**, 327–336 (2011).
16. Lee, S. S. et al. A systematic RNAi screen identifies a critical role for mitochondria in *C. elegans* longevity. *Nat. Genet.* **33**, 40–48 (2003).
17. Glenn, C. F. et al. Behavioral deficits during early stages of aging in *Caenorhabditis elegans* result from locomotory deficits possibly linked to muscle frailty. *J. Gerontol. A Biol. Sci. Med Sci.* **59**, 1251–1260 (2004).
18. Pelicioni, P. H. S. et al. Mild and marked executive dysfunction and falls in people with Parkinson's disease. *Braz. J Phys. Ther*. https://doi.org/10.1016/j.bjpt.2020.11.005 (2020).
19. Ibanez-Ventoso, C. et al. Automated analysis of *C. elegans* swim behavior using CeleST software. *J. Vis. Exp*. https://doi.org/10.3791/54359 (2016).
20. Burkewitz, K. et al. Neuronal CRTC-1 governs systemic mitochondrial metabolism and lifespan via a catecholamine signal. *Cell* **160**, 842–855 (2015).
21. Philip, N. S. et al. *Mos1* element-mediated CRISPR integration of transgenes in *Caenorhabditis elegans*. *G3* **9**, 2629–2635 (2019).
22. Paix, A. et al. High efficiency, homology-directed genome editing in *Caenorhabditis elegans* using CRISPR-Cas9 ribonucleoprotein complexes. *Genetics* **201**, 47–54 (2015).
23. Kwon, Y. J. et al. High-throughput biosorter quantification of relative mitochondrial content and membrane potential in living *Caenorhabditis elegans*. *Mitochondrion* **40**, 42–50 (2018).
24. Tsalik, E. L. & Hobert, O. Functional mapping of neurons that control locomotory behavior in *Caenorhabditis elegans*. *J. Neurobiol.* **56**, 178–197 (2003).
25. Berry, B. J. et al. Neuronal AMPK coordinates mitochondrial energy sensing and hypoxia resistance in *C. elegans*. *FASEB J.* **34**, 16333–16347 (2020).
26. Cox, J. et al. Accurate proteome-wide label-free quantification by delayed normalization and maximal peptide ratio extraction, termed MaxLFQ. *Mol. Cell Proteom.* **13**, 2513–2526 (2014).
27. Perez-Riverol, Y. et al. The PRIDE database resources in 2022: a hub for mass spectrometry-based proteomics evidences. *Nucleic Acids Res.* **50**, D543–D552 (2022).
28. Deutsch, E. W. et al. The ProteomeXchange consortium in 2020: enabling 'big data' approaches in proteomics. *Nucleic Acids Res.* **48**, D1145–D1152 (2020).
29. Perez-Riverol, Y. et al. PRIDE inspector toolsuite: moving toward a universal visualization tool for proteomics data standard formats and quality assessment of ProteomeXchange datasets. *Mol. Cell Proteom.* **15**, 305–317 (2016).

Acknowledgements

B.J.B. is supported by the Biological Mechanisms for Healthy Aging Training Grant National Institutes of Health (NIH)/National Institute on Aging T32 AG066574 and by NIH/NIA grant P30AG013280 to M.K. A.P.W. is supported by NIH grants (R01 NS092558 and R01 NS115906). S.P. is supported by a Deutsche Forschungsgemeinschaft grant (458246576) by two Longevity Impetus grants from Norn Group. We also acknowledge the W. M. Keck Microscopy Center and the Keck Center Manager and N. Peters for confocal microscopy access and training (NIH S10 OD016240).

Author contributions

B.J.B., M.K., S.P. and A.P.W. designed the research. B.J.B. performed the lifespans, imaging and analysis, healthspan experiments and data analysis. A.V. carried out lifespan and respiration experiments. A.M.E. carried out lifespan experiments. C.M. and C.L. carried out mass spectrometry. B.J.B. wrote the manuscript with input from M.K., S.P. and A.P.W.

Competing interests

B.J.B., S.P. and A.P.W. are listed as inventors on a patent application based on some of the work described here. The remaining authors declare no competing interests.

Additional information

Supplementary information The online version contains supplementary material available at https://doi.org/10.1038/s43587-022-00340-7.

Correspondence and requests for materials should be addressed to Shahaf Peleg or Andrew P. Wojtovich.

Peer review information *Nature Aging* thanks Liza Pon, Alex Soukas, and the other, anonymous, reviewer(s) for their contribution to the peer review of this work.

nature portfolio

Corresponding author(s): Peleg and Wojtovich

Last updated by author(s): Oct 3, 2022

Reporting Summary

Nature Portfolio wishes to improve the reproducibility of the work that we publish. This form provides structure for consistency and transparency in reporting. For further information on Nature Portfolio policies, see our Editorial Policies and the Editorial Policy Checklist.

Please do not complete any field with "not applicable" or n/a. Refer to the help text for what text to use if an item is not relevant to your study.
For final submission: please carefully check your responses for accuracy; you will not be able to make changes later.

Statistics

For all statistical analyses, confirm that the following items are present in the figure legend, table legend, main text, or Methods section.

n/a | Confirmed

- ☐ ☒ The exact sample size (*n*) for each experimental group/condition, given as a discrete number and unit of measurement
  A statement on whether measurements were taken from distinct samples or whether the same sample was measured repeatedly
- ☐ ☒ The statistical test(s) used AND whether they are one- or two-sided
  Only common tests should be described solely by name; describe more complex techniques in the Methods section.
- ☐ ☒ A description of all covariates tested
- ☐ ☒ A description of any assumptions or corrections, such as tests of normality and adjustment for multiple comparisons
- ☐ ☒ A full description of the statistical parameters including central tendency (e.g. means) or other basic estimates (e.g. regression coefficient) AND variation (e.g. standard deviation) or associated estimates of uncertainty (e.g. confidence intervals)
- ☐ ☒ For null hypothesis testing, the test statistic (e.g. *F*, *t*, *r*) with confidence intervals, effect sizes, degrees of freedom and *P* value noted
  Give P values as exact values whenever suitable.
- ☐ ☒ For Bayesian analysis, information on the choice of priors and Markov chain Monte Carlo settings
  For hierarchical and complex designs, identification of the appropriate level for tests and full reporting of outcomes
- ☒ ☐ Estimates of effect sizes (e.g. Cohen's *d*, Pearson's *r*), indicating how they were calculated
- ☒ ☐
- ☒ ☐

Our web collection on statistics for biologists contains articles on many of the points above.

Software and code

Policy information about availability of computer code

Data collection	Oxygen consumption data was collected using Oxygraph+ System (Hansatech Instruments Ltd). Confocal images were acquired using a Leica SP8X DMI6000 confocal microscope and Images were analyzed and prepared using Leica LASX Expert software and ImageJ. LC-MS/MS measurements were performed on an Ultimate 3000 RSLCnano system coupled to a Q-Exactive HF-X mass spectrometer (Thermo Fisher Scientific). Peptide identification and quantification was performed using MaxQuant (version 1.6.3.4).
Data analysis	Image J 1.53t, Prism 9.3.0, MaxQuant (version 1.6.3.4)

For manuscripts utilizing custom algorithms or software that are central to the research but not yet described in published literature, software must be made available to editors and reviewers. We strongly encourage code deposition in a community repository (e.g. GitHub). See the Nature Portfolio guidelines for submitting code & software for further information.

Data

Policy information about availability of data

All manuscripts must include a data availability statement. This statement should provide the following information, where applicable:

- Accession codes, unique identifiers, or web links for publicly available datasets
- A description of any restrictions on data availability
- For clinical datasets or third party data, please ensure that the statement adheres to our policy

All the data and accession codes supporting the findings are available in the main text, supplementary figures and tables. Proteomics data accession codes are listed in the main text.

Human research participants

Policy information about studies involving human research participants and Sex and Gender in Research.

Reporting on sex and gender	N/A
Population characteristics	N/A
Recruitment	N/A
Ethics oversight	Identify the organization(s) that approved the study protocol. N/A

Note that full information on the approval of the study protocol must also be provided in the manuscript.

Field-specific reporting

Please select the one below that is the best fit for your research. If you are not sure, read the appropriate sections before making your selection.

☒ Life sciences ☐ Behavioural & social sciences ☐ Ecological, evolutionary & environmental sciences

For a reference copy of the document with all sections, see nature.com/documents/nr-reporting-summary-flat.pdf

Life sciences study design

All studies must disclose on these points even when the disclosure is negative.

Sample size	Sample sizes were determined using previous publications. Data in figure 2 were calculated by previous publications from the Kaeberlein laboratory. Supplemental data were calculated by previous publications from the Peleg laboratory (for supplemetal figure 4).
Data exclusions	No data were excluded from the analyses.
Replication	Each experiment is composed of at least three technical and biological replicates. Each technical replicate can be composed of multiple animals or trials. The specific number of replicates and how an "N" is defined is described in the figure legends for each experiment.
Randomization	Experimental groups were determined for each genotype and animals were randomly assigned to treatment groups.
Blinding	The experimenter was blinded to the genotype or condition for behavioral assays only.

Reporting for specific materials, systems and methods

We require information from authors about some types of materials, experimental systems and methods used in many studies. Here, indicate whether each material, system or method listed is relevant to your study. If you are not sure if a list item applies to your research, read the appropriate section before selecting a response.

Materials & experimental systems

n/a	Involved in the study
☒	☐ Antibodies
☒	☐ Eukaryotic cell lines
☒	☐ Palaeontology and archaeology
☒	☐ Animals and other organisms
☐	☒ Clinical data
☒	☐ Dual use research of concern
☒	☐

Methods

n/a	Involved in the study
☒	☐ ChIP-seq
☒	☐ Flow cytometry
☒	☐ MRI-based neuroimaging

Animals and other research organisms

Policy information about studies involving animals; ARRIVE guidelines recommended for reporting animal research, and Sex and Gender in Research

Laboratory animals	Caenorhabditis elegans were used in this study and some strains were provided by the Caenorhabditis Genetics Center (CGC). Optogenetic strains were created from the N2 bristol wildtype and the WBM60 strain from CGC. Created strains were APW273 and APW312. The age of the animals are reported in the figure and figure legend, day 1 adult, day 4 adult and day 10 adult.
Wild animals	The study did not use wild animals
Reporting on sex	C. elegans are a largely hermaphroditic animal and only hermaphrodites were used in these studies.
Field-collected samples	The sutdy did not involve field-collected samples.
Ethics oversight	No ethical guidance was required for the invertebrate C. elegans. Experiments were approved by the University of Rochester Institutional Biosafety Committee.

Note that full information on the approval of the study protocol must also be provided in the manuscript.